

# Nucleon Structure Studies by Lepton Deep Inelastic Scattering

Fabienne KUNNE<sup>1\*</sup>

<sup>1</sup>CEA/IRFU/DPHn, CEA Saclay, F91 190 Gif/Yvette, France

\*E-mail: [Fabienne.kunne@cea.fr](mailto:Fabienne.kunne@cea.fr)

(Received February 25, 2019)

We present physics results obtained recently on the structure of the nucleon using lepton beams. The subjects discussed are: i) nucleon longitudinal spin structure with quark and gluon helicity measurements, ii) Semi-inclusive deep inelastic (SIDIS) results on hadron multiplicities for quark fragmentation function determination, iii) Transverse Momentum Dependent Distributions via SIDIS reactions and iv) Generalized Parton Distributions studies via Deep Virtual Compton Scattering and Meson Production. Data were taken at JLab (6 GeV electrons), HERMES (27 GeV electrons) and COMPASS (160/ 190 GeV muons).

**KEYWORDS:** Deep Inelastic Scattering, DIS, SIDIS, nucleon spin, quark and gluon helicity, quark fragmentation function, TMD, GPD.

## 1. Introduction

Extensive sets of data have been obtained in the last decade on nucleon structure studies via deep inelastic scattering (DIS). Experiments were held at Jefferson Lab (JLab) in US, at HERMES in DESY, Germany until 2007, and at COMPASS at CERN, using electron beams of 6 and 27 GeV for the two first facilities, and 160/190 GeV muon beam for COMPASS. The kinematic coverage was quite complementary (Fig.1). It will be complemented by the 12 GeV beam now in use at JLab and possibly later by the EIC electron ion collider. Results related to four physics topics are illustrated here: nucleon spin, quark fragmentation functions, transverse spin and transverse momentum dependences, and generalized parton distributions.

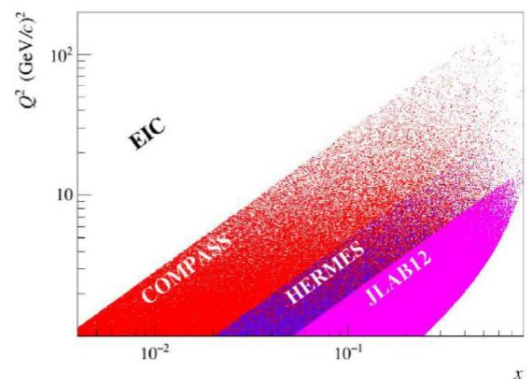


**Fig. 1.**  $x$ - $Q^2$  kinematic range for experiments and future project (EIC).

## 2. Nucleon Longitudinal Spin: quark and gluon helicities from DIS

A large experimental effort has been dedicated to study the spin structure of the nucleon, by measuring quark and gluon helicities in a longitudinally polarized nucleon.

The question raised was how the nucleon spin is distributed among its constituents, *i.e.*, what is the fraction of nucleon spin taken by the quark spin ( $\frac{1}{2} \Delta\Sigma$ ), the gluon spin ( $\Delta G$ ) and the total orbital angular momentum  $L$  to fulfill the sum rule:  $\frac{1}{2} = \frac{1}{2} \Delta\Sigma + \Delta G + L$ . Gluon and quark densities are measured via DIS and photon-gluon fusion (PGF) processes respectively (Fig.2 a and b). To access the helicities rather than the densities, one has to measure the spin asymmetries of cross sections, between parallel and anti-parallel spin states, using polarized lepton beams and polarized nucleon targets.

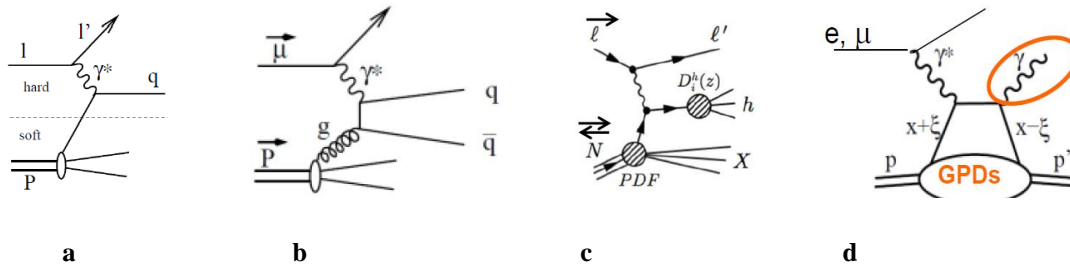


**Fig. 2.** The processes (from left to right): **a)** Inclusive Deep Inelastic Scattering (DIS), **b)** Photon Gluon Fusion (PGF), **c)** Semi-Inclusive DIS (SIDIS) and **d)** Deep Virtual Compton Scattering (DVCS).

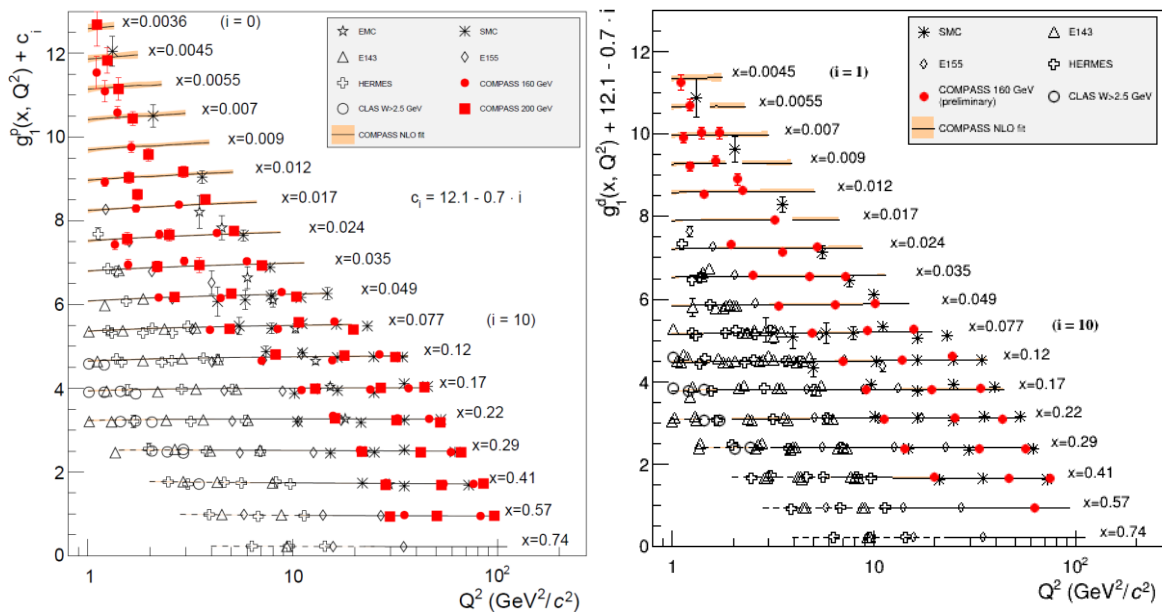


**Fig. 3.** World data spin structure function  $g_1(x, Q^2)$  of the proton (**Left**) and deuteron (**Right**);  $W > 5 \text{ GeV}$  [1].

World data on polarized DIS ( $Q^2 > 1 \text{ GeV}^2$ ;  $W > 5 \text{ GeV}$ ) on proton and deuteron cover more than two decades in  $x$  and in  $Q^2$  (Fig.3). They were used in global QCD Next-To-Leading Order (NLO) fits to polarized Parton Distribution Functions (PDF), using assumptions for initial functional forms at a starting  $Q^2$ . Note that  $\Delta\Sigma$  and  $\Delta G$  are coupled via the  $x$ - $Q^2$  DGLAP evolution equations. We show results from such a fit [1] (Fig.4 left) based on DIS data only.  $\Delta G$  is not well constrained, with positive and negative solutions allowed.  $\Delta\Sigma$ , well constrained in the valence region, still suffers from an uncertainty at small  $x$  due to the bad knowledge of the functional forms (of  $\Delta G$  mainly). Thus, the

resulting integral  $\Delta\Sigma=0.31(5)$ , in fair agreement with other NLO global fits, has a large uncertainty in spite of the precision and density of  $g_1$  data. To better constrain  $\Delta G$ , fits [2] have to include polarized pp data from RHIC.

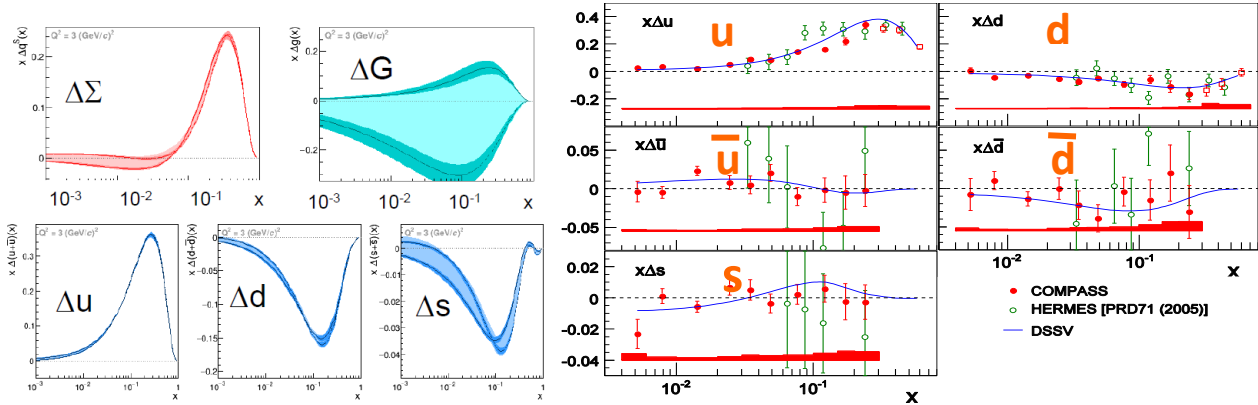


**Fig. 4.** Left: Polarized parton distributions from the fit to  $g_1$  world data at  $Q^2=3 \text{ GeV}^2$ , for singlet and gluon (Top) and u, d and s quark flavors (Bottom) [1]; Right: Polarized parton distributions per flavor, from polarized SIDIS: HERMES[3] (open points) and COMPASS[4] (full points) data, and DSSV fit (blue line).

Fig.4 right shows polarized parton distributions per flavor obtained at LO from SIDIS (Fig.2c) data [3,4], where the outgoing hadron ( $\pi, K$ ) tags the flavor of the struck quark via quark fragmentation functions (see below). The gluon polarization  $\Delta G/G$  was extracted at LO from PGF (Fig.2b) events. Results (Fig.5) are compatible with the above  $\Delta G>0$  solution, and with the DSSV++ fit [2] based on pp data and concluding to  $\Delta G\sim 0.2$  for the integral between  $x=0.05$  and  $0.2$ .

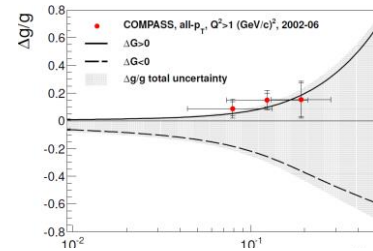


**Fig. 5.**  $\Delta G/G(x)$  direct extraction in hadron production [5].

### 3. SIDIS Hadron Multiplicities for Quark Fragmentation Functions

Fragmentation functions (FF) are universal non-perturbative objects, needed in particular for the polarized parton extraction from SIDIS data mentioned earlier. FFs, noted as  $D_q^h$ , represent the probability of a quark  $q$  to hadronize into a hadron  $h$ . The FFs are not well determined yet, in particular for the strange quark sector. By measuring hadron multiplicities in SIDIS, one accesses a convolution of PDFs and FFs. While PDFs depend on  $x$ , FFs depend on  $z$ , the fraction of energy taken by the outgoing hadron. By measuring kaon multiplicities, one accesses typically  $s(x, Q^2) D_s^K(z, Q^2)$ . Pion and kaon multiplicities [6,7] constitute an important input to global NLO QCD analyses : recent QCD fits [8,9] show that incorporating the latest kaon SIDIS data [7] (more than 600 points) changes significantly the flavor decomposition of FFs compared to earlier fits.

For kaons, with an isoscalar target, the sum of  $K^+$  and  $K^-$  multiplicities has a simple expression at LO, showing a sensitivity to the strange quark FF  $D_s^K$  at low  $x$  and to the non-strange one at high  $x$ . For this sum, COMPASS data are well above HERMES ones (Fig.6 left), however measured at different kinematics. Note that Accardi et al. [10] have

proposed target mass corrections to explain part of this discrepancy. Also, additional recent data [11] on the ratio of  $K^-$  to  $K^+$  multiplicities at high  $z$  fall well below pQCD

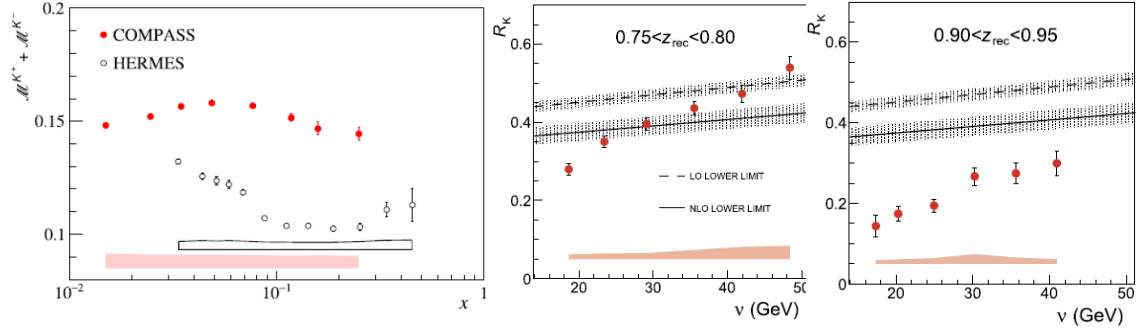


**Fig. 6. Left:** Sum of  $z$ -integrated kaon multiplicities versus  $x$ ; the bands are systematic uncertainties. **Middle and Right:** Ratio of  $K^-$  to  $K^+$  multiplicities measured at high  $z$ , versus  $\nu$ , the virtual photon energy, in two different  $z$  bins. The curves correspond to theory lower limit expectation at LO and NLO.

expectations, especially at low values of the energy of the virtual photon (Fig.6 middle and right). This suggests to take into account the phase space available for hadronization in further theoretical calculations. The disagreement could happen at lower  $z$  for experiments covering lower  $\nu$ . This could help explain the disagreement between the two sets of data.

#### 4. Transverse Spin and Transverse Momentum Dependence

Another important variable in the study of nucleon structure is  $p_T$ , the transverse momentum of the outgoing hadron in SIDIS. The  $p_T$  dependence of the observables results from the intrinsic transverse momentum  $k_\perp$  of the quark and the  $p_T$  generated in the quark fragmentation. Several global analyses of all SIDIS, Drell-Yan and Z production data aim at parametrizing the  $x$  dependence of  $\langle k_\perp \rangle$ . Fig. 7 shows an example of SIDIS multiplicity data [12]. Fig.8 shows the resulting  $\langle k_\perp \rangle$  obtained in one of the global fits [14].

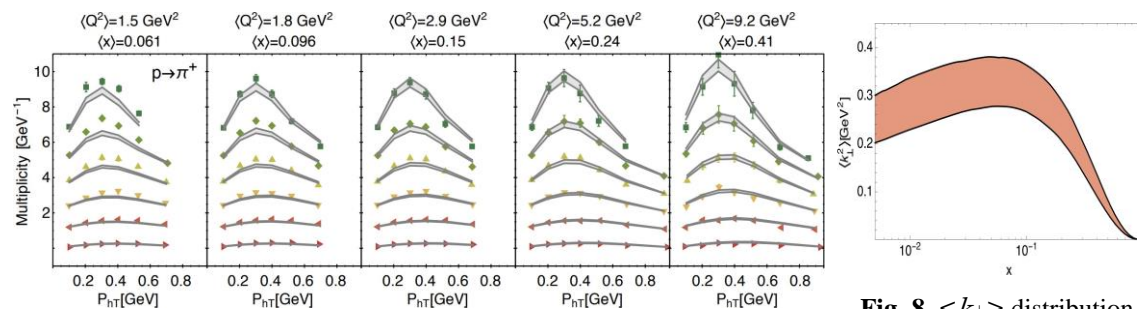


**Fig. 7.** Theory [13] and data for  $p_T$  dependent  $\pi$  multiplicity (here HERMES [12], proton target). Figure taken from [13].

**Fig. 8.**  $\langle k_\perp \rangle$  distribution vs  $x$ , obtained from a global fit [14].

Transverse momentum dependent PDFs (TMD PDFs [15-17] and references therein) constitute an important tool to study nucleon structure. The most famous TMD PDFs, the Siverson function and the transversity (measured via Collins effect), can be accessed in

SIDIS using a transversely polarized target, via azimuthal distributions of the hadron. Several azimuthal asymmetries are measured simultaneously. Among them, the Collins asymmetry results from a correlation between the outgoing hadron direction and the quark transverse spin. The Sivers asymmetry represents a correlation between the nucleon spin and the quark transverse momentum  $k_{\perp}$ . Fig.9a-left shows an example of data on the Sivers asymmetry for  $\pi$  and K SIDIS on a proton target [18, 19]. Fig.9a-right shows the first moment of the Sivers TMD for various quark flavors extracted from a global fit [20] to all data. Fig.9b shows the transversity TMD extracted from a global fit [21].

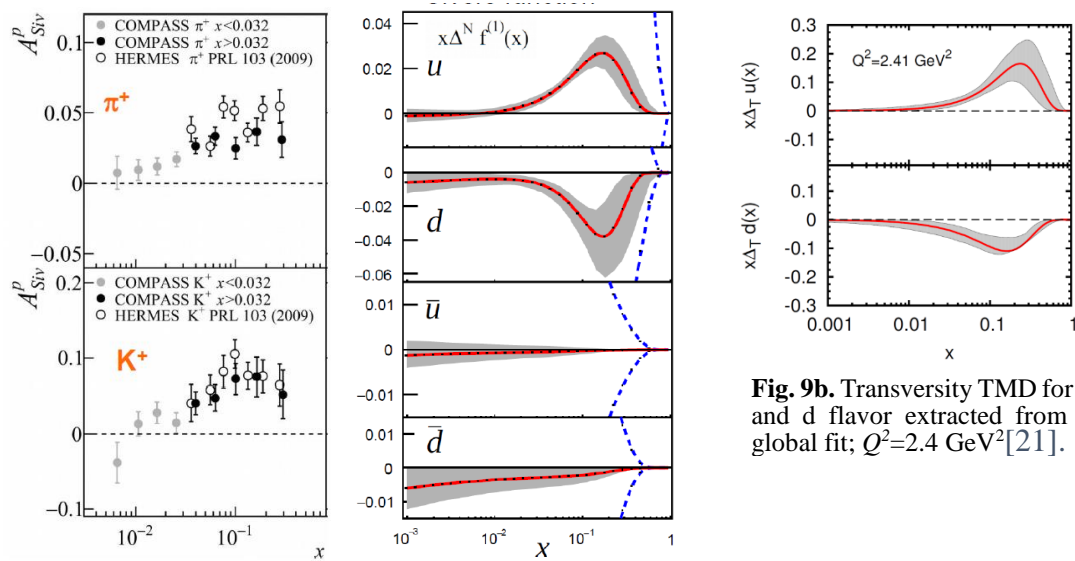


**Fig. 9b.** Transversity TMD for  $u$  and  $d$  flavor extracted from a global fit;  $Q^2=2.4 \text{ GeV}^2$ [21].

**Fig. 9a. Left:** Sivers asymmetry for  $\pi$  and  $K$  produced via SIDIS on a proton. **Right:** Extracted first moment of the Sivers functions at  $Q^2=2.4 \text{ GeV}^2$ [20].

Overall, recent results on TMDs are characterized by an unprecedented precision, covering many observables in a wide kinematic range. As an illustration, we show results for one of the many others azimuthal asymmetries, here obtained from SIDIS data on a longitudinally polarized proton, for production of positive hadrons, negative hadrons and  $\pi^0$  (Fig.10). When including those data in global QCD fits, the improvement is spectacular [24] (narrow green bands instead of wide blue ones in Fig.10 left and middle).

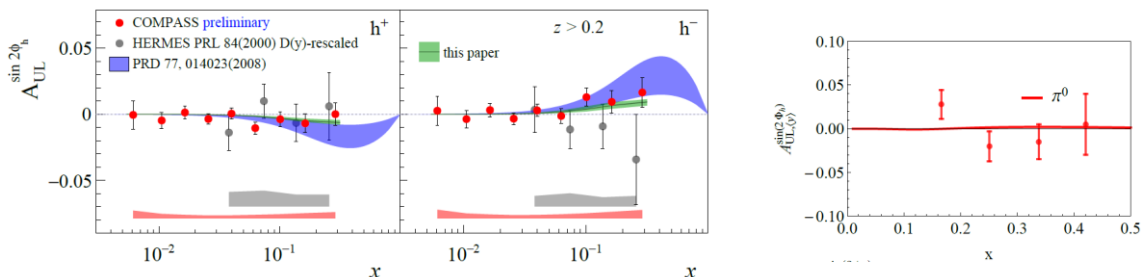


**Fig. 10.** The azimuthal ( $\sin 2\phi$ ) asymmetry  $A_{UL}(x)$  for  $h^+$  (Left),  $h^-$  (Middle) and  $\pi^0$  (Right) production in SIDIS at HERMES [22], COMPASS and JLab CLAS [23] compared to old (blue band) and new [24] global fits. Figures taken from [24]. Grey and pink bands are systematic errors associated to data.

Finally, we should mention a new approach to TMDs using weighted asymmetries [25]. Weighting adequately the events, e.g. with  $p_T/zM$ , in the evaluation of the asymmetries, one can access a product of the integrals of moments of TMDs and FFs, instead of a convolution. Thus the first moment of the Sivers or other TMDs can be extracted without assumption on the  $k_T$  dependence of the observables, making a decisive progress.

### 5. Generalized Parton Distributions: DVCS and DVMP measurements

The Generalized Parton Distribution (GPD) formalism is described in detail in Ref. [26]. The physics goals of the measurements are a 3D mapping of the partons in the nucleon and a determination of their orbital angular momentum. We give here only examples of results obtained so far in Deep Virtual Compton Scattering (DVCS) and Deep Vector Meson Production (DVMP). The bulk of data on DVCS and DVMP come from JLab experiments. Additional ones come from HERMES, COMPASS, H1 and ZEUS.

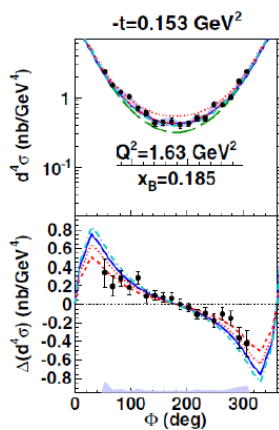


Fig. 11. CLAS data on DVCS cross sections [27].

Fig. 11 shows a sample of JLab CLAS data [27] on differential cross sections and “beam-spin difference” of cross sections in a given  $(x, Q^2, t)$  bin. The impressive amount of very precise data obtained in a large kinematic range allows to extract

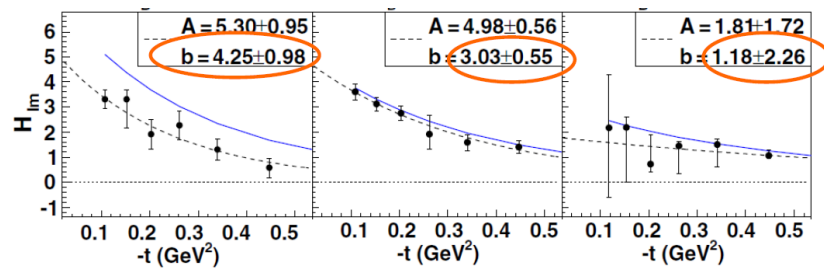


Fig. 12. Fit of CLAS cross section data to CFF  $\text{Im}(H)$  at three  $x$  values [27].

the  $H$  Compton Form Factor (CFF, physics quantity needed to access a GPD). Fig.12 shows  $\text{Im}(H)$  vs the transfer  $t$ , for three  $x$  bins. In each  $x$ -bin, the  $b$  slope is extracted, leading to the proton transverse size. Although still limited in precision on  $b$ , the results tend to indicate a shrinking size vs  $x$ . Other examples of measurements of transverse sizes are shown in Fig. 13 for the proton [28] and in Fig.14 for He [29].

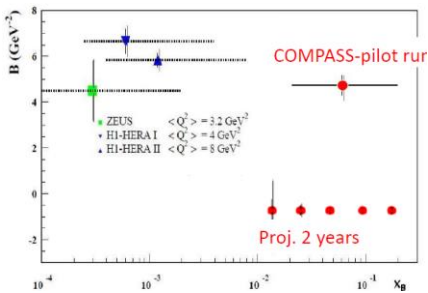


Fig. 13.  $B$  parameter linked to proton transverse size; HERA and COMPASS data [28] plus projections.

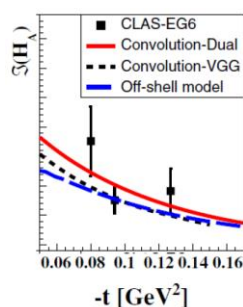
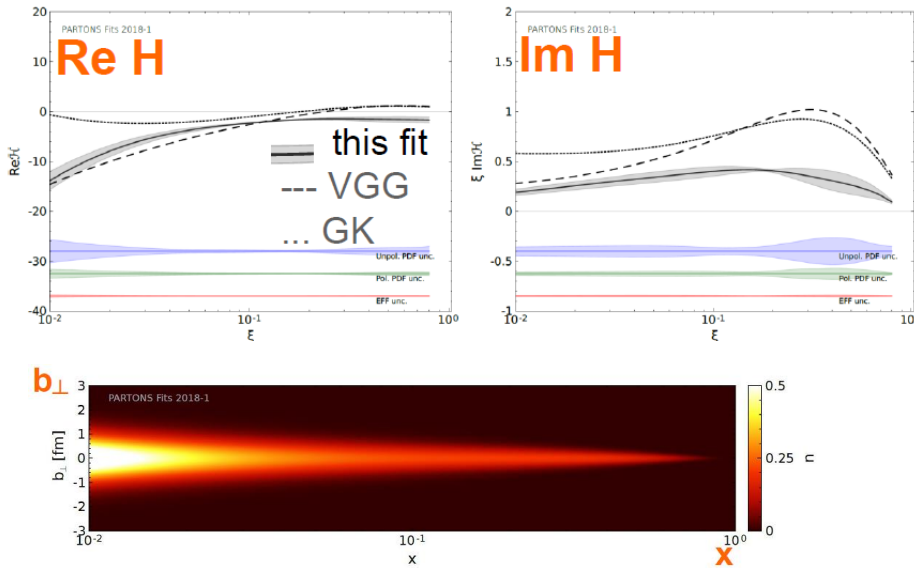


Fig. 14.  $\text{Im}(H)$  vs  $t$  for He, CLAS data [29].

The few results presented here are only a tiny illustration of the very large set of existing data points (e.g., more than 4000 for DVCS on the proton). To reach the goal of extracting the CFFs, those data have to be treated in global analyses. We show here an example of such a fit [30] based on 2600 data points, with some

additional constraints on GPDs (like PDFs, elastic form factors, limits at  $x \rightarrow 1 \dots$ ). Fig.15 shows the extracted CFF H, compared to previous extractions with less data, as well as a first glimpse on the position of the up quarks in the proton vs  $x$ .



**Fig. 15. Top:** Re and Im parts of CFF H, from a global fit [30] of DVCS data on the proton. **Bottom:** Correlation between transverse position of up quarks and  $x$  from the same fit.

In addition to DVCS data on proton, neutron, deuteron or light nuclei, measurements exist on the DVMP process, where the outgoing particle is a vector meson instead of a photon. Fig.16 shows results for  $\pi^0$  and  $\eta$  [31] exclusive production (DVMP). Fig.17 shows for the first time a clear Rosenbluth separation of  $\sigma_T$  and  $\sigma_L$  for  $\pi^0$  exclusive production [32].

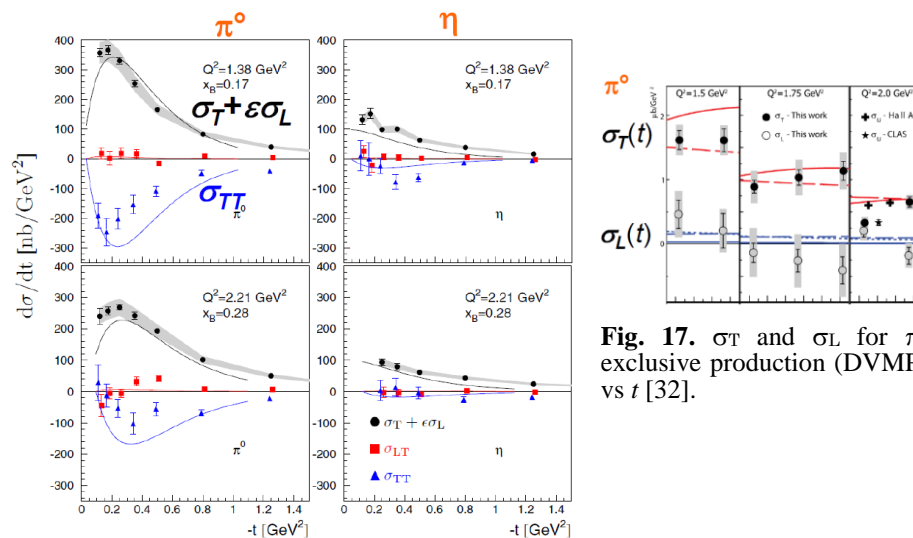


**Fig. 16.**  $\sigma_T + \epsilon\sigma_L$  for  $\pi^0$  and  $\eta$  DVMP vs  $t$  [31].

**Fig. 17.**  $\sigma_T$  and  $\sigma_L$  for  $\pi^0$  exclusive production (DVMP) vs  $t$  [32].

## 6. Conclusion

A few highlights on the main physics results obtained recently on the structure of the nucleon using lepton beams have been presented. They cover the subjects of i) nucleon longitudinal spin structure with quark and gluon helicity measurements, ii) SIDIS hadron multiplicities for quark FF determination, iii) TMDs via SIDIS reactions and iv) GPD studies via DVCS and DVMP reactions. The results come essentially from experiments having used JLab 6 GeV, HERMES 27 GeV and COMPASS 160/ 200 GeV lepton beams. They will be completed in the future by JLab 12 GeV data, and hopefully future EIC data.

## References

- [1] COMPASS Collab., PLB **753** (2016) 18
- [2] DSSV++ Collab., PRL **113** (2014) 012001
- [3] HERMES Collab, PRD **71** (2005) 012003
- [4] COMPASS Collab., PLB **693** (2010) 227
- [5] COMPASS Collab, DG LO EPJC **77** (2017) 209
- [6] HERMES Collab., Phys. ReD. **B89** (2014) 097101
- [7] COMPASS PLB **767** (2017) 133
- [8] DEHSS Collab., D. De Florian et al., PRD **95** (2017) 094019
- [9] N.Sato et al., JAM18, Proceedings of SPIN2018 conference
- [10] J. Guerrero and A. Accardi, PRD **97** (2018) 114012
- [11] COMPASS Collab., PLB **786** (2018) 390
- [12] A. Bacchetta et al., arXiv :1703.10157
- [13] HERMES Collab., Phys. Rev. **D87** (2013) 074029
- [14] A. Bacchetta et al., JHEP **06** (2017) 081
- [15] P. Mulders and R. Tangerman, Nucl. Phys.**B461**(1996)197; Erratum Nucl. Phys. **B484**(1997)538
- [16] A. Bacchetta et al., JHEP **02** (2007) 093
- [17] D. Boer and P. J. Mulders, Phys. Rev **D57** 5780 (1998)
- [18] HERMES Collab., PRL **103** (2009) 152002
- [19] COMPASS COLLAB., PLB **744** (2015) 250
- [20] M. Anselmino et al., JHEP **04** (2017) 046
- [21] M. Anselmino et al., PRD **87** (2013) 094019
- [22] HERMES Collab., PRL**84** (2000) 4047
- [23] S. Jawalkar et al., CLAS Collab., arXiv :1709 :10054
- [24] S. Bastami et al., arXiv: 1807.10606
- [25] COMPASS Collab., Nucl. Phys. **B940**(2019) 34
- [26] B. Pasquini, contribution to this conference.
- [27] K. Jo et al., PRL **115** (2015) 212003
- [28] COMPASS Collab., CERN-EP/2018-**016**, arXiv: 1802.02739, subm. to PLB
- [29] M. Hattawy et al., PRL **119** (2017) 202004
- [30] H. Moutarde et al., arXiv:1807.07620
- [31] I. Bedlinskiy et al., PRC **95** (2017) 035202
- [32] M. Defurne et al., PRL **117** (2016) 262001